

# Model Support for an Out-Reactor-Instrumented-Defected-Fuel-Experiment to Validate the RMC Fuel Oxidation Model

A.D. Quastel<sup>1</sup>, E.C. Corcoran<sup>1</sup>, B.J. Lewis<sup>1</sup>, W.T. Thompson<sup>1</sup>,  
C. Thiriet<sup>2</sup>, G. Hadaller<sup>3</sup>

<sup>1</sup>Chemistry and Chemical Engineering Department, Royal Military College of Canada, P.O. Box 17000 Station Forces, Kingston, Ontario, Canada, K7K7B4

<sup>2</sup>Atomic Energy of Canada Limited, Chalk River Laboratories, Chalk River, Ontario, Canada, K0J1J0

<sup>3</sup>Stern Laboratories Inc., 1590 Burlington Street East, Hamilton, Ontario, Canada, L8H3L3

## Abstract

An out-reactor fuel oxidation experiment with controlled parameters is being planned to provide important data for validation of a mechanistic fuel oxidation model. In support of this experimental planning, fuel oxidation 2D and 3D models are presented in this paper. The model results indicate that increased defect surface area increases the maximum oxygen stoichiometric deviation in the UO<sub>2</sub> fuel pellet. Model predictions indicate that a stoichiometric deviation of 0.0230 will result within one week of heating a defective fuel element with a 20-mm<sup>2</sup> sheath defect. The model also predicts that doubling the heating time increases fuel oxidation by 49%. A 2D  $r$ - $\theta$  fuel oxidation model capable of estimating the required electrical linear power is also presented.

## 1. Introduction

Fuel oxidation in defective fuel has been an area of continued research. A fuel oxidation model has been developed that describes this phenomena [1] but a controlled experiment has yet to be performed to validate and possibly improve the model. In a CANDU nuclear reactor the UO<sub>2</sub> fuel is separated from the reactor coolant using Zircaloy sheathing (see Figure 1). The fuel element sheathing prevents the release of fission products into the coolant and protects the fuel from being oxidized. On occasion, a small hole or crack can occur in the sheathing during reactor operation as a result of debris fretting, pellet-cladding interaction or because of manufacture defects. Such sheath breaches allow coolant (heavy water) to enter the fuel element and make direct contact with the fuel [2,3] leading to fuel oxidation.

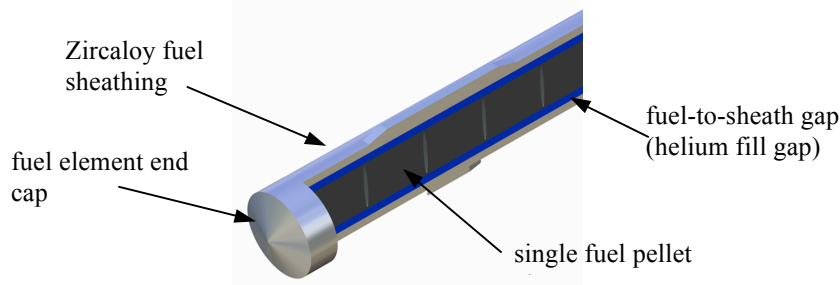


**Figure 1: A single CANDU-6 fuel element cut-away. The dimensions of the gap between fuel pellets and the sheath-to-fuel gap are not to scale.**

As the fuel is oxidized, the fuel thermal conductivity will be degraded resulting in higher fuel temperatures. Moreover, in hyper-stoichiometric fuel, the melting temperature will be reduced leading possibly to centreline fuel melting in high-powered elements, particularly during accident conditions [4-7]. Fission product release will also be enhanced by a greater mobility in the hyper-stoichiometric fuel [8].

A mechanistic fuel oxidation model for defected fuel was previously developed at the Royal Military College of Canada [1]. This model has been extended in preparation for comparison to validation experimentation. An Out-Reactor Instrumented Defective Fuel Experiment currently is being planned by AECL-CRL (Atomic Energy of Canada Limited - Chalk River Laboratories) at STERN Laboratories to measure, in real-time, the fuel element temperature at various radial and axial locations and possibly the oxygen potential at each end of the fuel element. The out-reactor test will provide important data for the validation of the RMC defective fuel oxidation model.

Previous experiments have been conducted to investigate various aspects of defective fuel. Lewis *et al* [3] and Hüttig *et al* [9] investigated fission product release, Une *et al* [10] measured post irradiation fuel oxidation, Limbäck *et al* [11] and Cheng *et al* [12] investigated secondary fuel degradation with in-situ centreline fuel temperature measurements and hydrogen gas pressure measurements in the later experiment. The motivation for the proposed experiment is that fuel oxidation has never been investigated experimentally at both high coolant pressure ( $\sim 10$  MPa) and reactor temperatures while simultaneously measuring in-situ fuel temperatures and possibly the oxygen potential. The proposed experiment would also incorporate highly controlled test parameters such as the onset of a sheath defect (of a specific size), heating duration and power settings. The test would thus be able to measure the fuel thermal conductivity degradation in real time. Results would be used to validate key aspects of the RMC fuel oxidation model. The model could then be incorporated into fuel performance codes for normal and accident condition analysis in order to specifically address the Canadian Nuclear Safety Commission (CNSC) issues on the possibility of fuel centreline melting in defective fuel during normal and power-pulse situations [13]. An experimentally demonstrated fuel oxidation model is applicable not only to CANDU reactors but also to PWRs and BWRs, which constitute about 75% of all world power reactors.

This paper provides 3D fuel oxidation modelling in support of the design for an out-reactor fuel oxidation experiment to define suitable test parameters and materials selection. This paper also attempts to investigate possible fuel oxidation with steam ingress in the pellet-pellet interface gap.

## 2. Proposed Out-Reactor-Instrumented-Defective-Fuel-Experiment Setup

The out-reactor test facility at STERN Laboratories will include a small self-contained coolant loop capable of operating at CANDU reactor conditions. This loop is designed to run at up to 10 MPa inlet pressure and a normal coolant temperatures to 310°C. A laboratory data acquisition system will monitor the loop and test-fuel simulator instrumentation.

A fuel element would have 31 fuel pellets with an axial clearance of 1 to 3 mm. Typical fuel sheath defect surface areas can range from about 1 to 13 mm<sup>2</sup> [7,14]. At a chosen time after a conditioning period, an artificial slit defect can be initiated in-situ in the sheath. The breached sheath will expose the fuel to water at a temperature of approximately 300°C and a pressure of approximately 10 MPa.

Each test pellet will be about 16-mm in length and 12-mm in diameter. The test pellets will include a central hole to accommodate an electrical heating element. Temperature measurement of the test fuel will be performed with thermocouples at three radial positions in the test pellet as indicated in Figure 2.

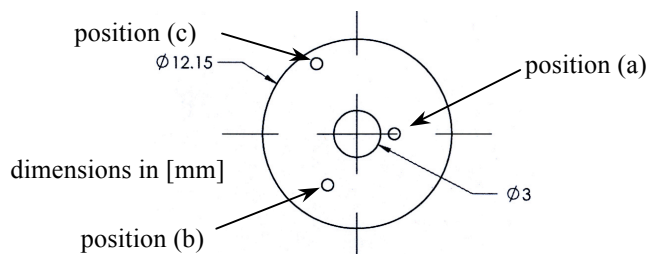


**Figure 2: Radial cross section of test pellet with drill holes. The 3-mm diameter central hole is for the electrical heating wire. The smaller holes provide access for thermocouples and thermocouple wires. Thermocouple sites at: a) close to the pellet centre and near the heating element, b) between the pellet centre and pellet outer surface and c) near the outer surface of the pellet.**

An electrical heating wire will run through the entire central length of the test fuel element. This heating technique has been successfully employed in the past by Oguma [15]. The heater element wire will be approximately 3-mm in diameter. Tantalum (Ta) wire is a good candidate for the heating element but it needs to be coated with a noble metal, such as iridium (Ir), to prevent Ta oxidizing in the steam environment. Consideration is given also to the Ta-Ir eutectic temperature of 1953°C [16]. In order to prevent electric arcing between the heating element wire and the fuel pellets, the Ir-coated Ta heating wire will be surrounded by an electrical-insulating material such as alumina ( $\text{Al}_2\text{O}_3$ ) or hafnia ( $\text{HfO}_2$ ), which are both considered in the current work.

Measurement of the oxygen potential, or the O/M ratio, at several radial locations in the test fuel pellet will be required for validating the fuel oxidation model. The first post experiment method (a macroscopic approach) is the traditional Coulometric Titration (CT) method [14] employed previously at AECL-CRL to measure the average O/M ratio of spent CANDU fuel, which has a sensitivity of  $x = 0.01$  in  $\text{UO}_{2+x}$ . The second post experiment method (a microscopic approach) is using Wavelength Dispersive X-Ray (WDX) [17]. Preliminary tests will be performed to estimate the measurement sensitivity.

### 3. Fuel Oxidation Model Theory

The model used to produce results presented in this paper is based on the conceptual model of Higgs [1,18]. The model describes the fuel oxidation processes that occur within a defective fuel element operating under normal conditions. The model was modified for the current study to represent an inner-surface heated and unirradiated fuel element in the out-reactor experiment. The model includes a heat conduction equation, a gas transport equation and an oxygen diffusion equation, all coupled together as discussed in the following section.

#### 3.1 Mechanistic Model Fuel Oxidation

In the mechanistic model [1] a treatment is required for both gas phase and solid-state diffusion, which are controlled by temperature-dependent reactions. This necessitates knowledge of the temperature distribution in the fuel element. Hydrogen (H<sub>2</sub>) and steam (H<sub>2</sub>O) are specifically considered in this treatment for the out-reactor experiment.

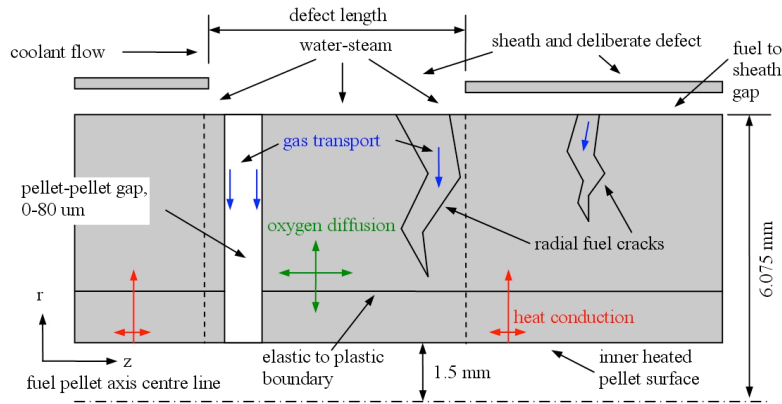


**Figure 3: A 2D  $z$ - $r$  representation of test fuel pellet. Heat conduction, gas transport in cracks and oxygen diffusion in the fuel are modelled in this treatment. The width of the defect, not shown, is 1-mm.**

Figure 3 depicts an axial cross section of a test fuel element. The cracks that will appear in the fuel pellets are a result of fuel thermal expansion [15,19], and is an important model parameter. Below the elastic-plastic boundary, cracks will initially appear but will later self heal [20,21]. The temperature at which this transition is assumed to occur in the model is 1523 K, though in reality it occurs over a range of temperatures [15,21]. Figure 3 depicts a deliberate sheath defect which is 1-mm wide (into the page) and 20-30 mm long in the axial  $z$ -direction.

The initial hydrogen molar fraction,  $q$ , at the defect and in the volume of the radial assumed cracks directly under the defect site, is assumed to be  $4.1 \times 10^{-6}$  moles  $m^{-3}$ . This value is the hydrogen mole fraction of the coolant in reactor [1] and is used in the current model.

The generalized mass balance equation for oxygen transport in the fuel matrix is given by Eq. 1,

$$c_u \frac{\partial x}{\partial t} = c_u \nabla \cdot \left( D \left( \nabla x + x \frac{Q}{RT^2} \nabla T \right) \right) + \sigma_f R_f^{react} \quad (1)$$

where

$$D = 2.5 \times 10^{-4} \cdot \exp(-16400/T) \text{ m}^2 \text{ s}^{-1} \quad (2)$$

and  $x$  is the oxygen deviation from stoichiometry in the uranium oxide matrix ( $\text{UO}_{2+x}$ ),  $c_u$  is the molar density of uranium,  $R$  is the universal gas constant,  $T$  (in K) is temperature,  $\sigma_f$  is the pellet average ratio of crack area to fuel volume,  $R_f^{react}$  is the rate of reaction for either fuel oxidation or reduction in moles O or  $\text{H}_2 \text{ m}^{-2}\cdot\text{s}^{-1}$ .  $D$  in Eq. 2 is the diffusion coefficient for oxygen interstitials, which is a function of temperature ( $T$  in K) [1].  $Q$  in the molar effective heat transport given by Eq. 3, (where  $x$  is the stoichiometric deviation value). A Neumann boundary condition for the oxygen stoichiometric deviation is taken as zero at all external geometric boundaries.

$$Q = -3.5 \times 10^{34} \exp(-17(4 + 2x)) \text{ J mol}^{-1} \quad (3)$$

The kinetic reaction rate,  $R_f^{react}$ , for fuel oxidation is given by Eq. 4:

$$R_f^{react} = c_u \alpha \sqrt{(1-q)p_t} (x_e - x) \quad (4)$$

where  $\alpha$  is the rate coefficient for the surface-exchange of oxygen ( $\alpha = 0.365 \exp(-23500/T)$  (K))  $\text{m s}^{-1}$  [1]). At the pellet surface  $p_t$  is the total system pressure in atmospheres,  $q$  is the hydrogen mole fraction,  $x$  is stoichiometric deviation, and  $x_e$  is the equilibrium stoichiometry deviation based on the local oxygen potential of the gas in the fuel cracks [1].

Hydrogen is contributed to the gas environment in the fuel cracks by the fuel-oxidation reaction. The cracked fuel is assumed to have a porosity  $\varepsilon$ . The mass balance for the hydrogen molar concentration,  $qc_g$ , in the fuel cracks is given in general form by Eq. 5 where  $c_g$  is the total molar

$$\varepsilon \frac{d(qc_g)}{dt} = \varepsilon \nabla \cdot (c_g D_g \nabla q) + \sigma_f R_f^{react} \quad (5)$$

concentration of gas in  $\text{mol m}^{-3}$  and  $c_g D_g$  is the steam diffusivity quantity in  $\text{mol m}^{-1} \text{ s}^{-1}$ .

Eq. 5 is applicable only in the domain above the elastic-plastic boundary and only under the defect site (see dashed lines in Figure 3). Treatment of the hydrogen mole fraction along the fuel-to-sheath gap is not included in the current model since previous work indicate that it is not a dominant contributing factor to fuel oxidation. The temperature profile in the fuel element is obtained from the solution of the general time-dependent heat conduction equation, Eq. 6,

$$\rho_s C_p \frac{\partial T}{\partial t} = \nabla \cdot (k \nabla T) + Q_v \quad (6)$$

where  $\rho_s$  is the fuel density,  $C_p$  is the specific heat of the fuel,  $k$  is the thermal conductivity of the fuel and  $Q_v$  is the volumetric heat source term of the nuclear fuel. In the current model, the  $Q_v$  term is set to zero and replaced by a boundary condition for the given heater condition. Specifically, the temperature of the  $\text{UO}_2$  surface adjacent to the heater in the centre of the fuel pellet is set to a given temperature.  $C_p$  and  $k$  are both functions of  $T$  and  $x$ .

### 3.2 2D and 3D Fuel Oxidation Model

In this paper, the fuel oxidation model is solved for both 2D and 3D geometries. The 2D geometries are less computationally expensive; however this representation tends to over-predict the extent of fuel oxidation as the defect size increases. The 3D geometries are more computationally expensive but represent the extent of fuel oxidation for the actual size of defect.

In Figure 4, the green area on the sheath represents a 'continuous slit defect' along the axis of the fuel element in  $r-\theta$  polar coordinates. The purple area is another possible 2D model representation of a 'ring defect' in  $r-z$  polar coordinates (as considered in previous models [1]). The yellow area is a true representation of the sheath defect in the 3D model.

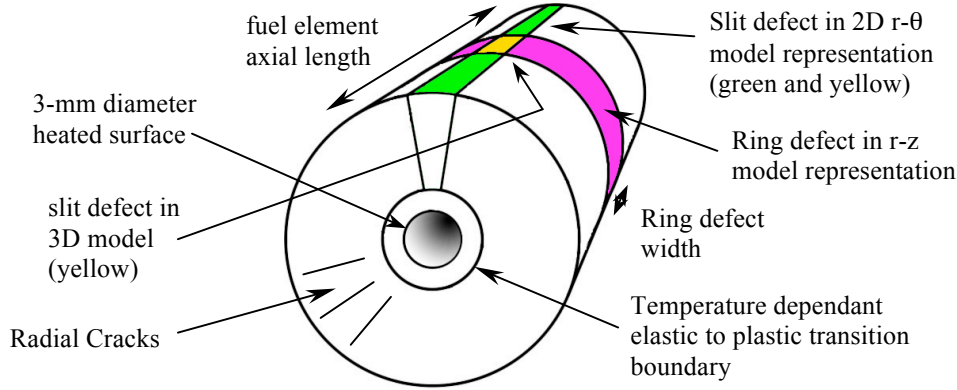


**Figure 4: 3D and 2D model defect representations; green area is a sheath defect in a 2D  $r-\theta$  model, purple represents a sheath defect in a 2D  $r-z$  model (not used here), and yellow represents a defect in a 3D model.**

In 3D, the oxygen transport in the solid fuel matrix occurs in all directions (though it is dominant in the radial direction due to the high temperature gradient), so Eq. 1 becomes:

$$c_c \frac{\partial x}{\partial t} = c_c \left[ \frac{1}{r} \frac{\partial}{\partial r} \left( rD \left( \frac{\partial x}{\partial r} + x \frac{Q}{RT^2} \frac{\partial T}{\partial r} \right) \right) + \frac{1}{r} \frac{\partial}{\partial \theta} \left( D \left( \frac{1}{r} \frac{\partial x}{\partial \theta} + x \frac{Q}{RT^2} \frac{1}{r} \frac{\partial T}{\partial \theta} \right) \right) + \frac{\partial}{\partial z} \left( D \left( \frac{\partial x}{\partial z} + x \frac{Q}{RT^2} \frac{\partial T}{\partial z} \right) \right) \right] + \sigma_f R_f^{react} \quad (7)$$

In the 2D  $r-\theta$  model, the equation simplifies by removing the  $z$ -polar coordinate term. Generally, if temperature is independent of  $\theta$  and  $z$  then the second and third diffusion terms simplify. But, in reality, these terms will not cancel out in the vicinity of thermocouples and thermocouple-drilled holes, and when consideration is made of the varying fuel thermal conductivity that is dependent on the degree of fuel oxidation.

Hydrogen gas transport in the fuel cracks is considered in the radial and azimuthal directions, though it too will be dominant in the radial direction since the diffusivity quantity is a function of temperature. Thus, the differential equation for the hydrogen mole fraction  $q$  (Eq. 5) in the cracked  $\text{UO}_2$  solid becomes:

$$\epsilon c_g \frac{\partial q}{\partial t} = \frac{\epsilon}{\tau^2 r} \left[ \frac{\partial}{\partial r} \left( r c_g D_g \frac{\partial q}{\partial r} \right) + \frac{\partial}{\partial \theta} \left( \frac{c_g D_g}{r} \frac{\partial q}{\partial \theta} \right) \right] + \sigma_f R_f^{react} \quad (8)$$

where  $t$  is time and  $\tau$  is tortuosity and the  $z$ -polar component is neglected.

The heat equation (Eq. 6) in 3D without a volumetric heat source term becomes:

$$\rho_s C_p \frac{\partial T}{\partial t} = \frac{1}{r} \frac{\partial}{\partial r} \left( r k \frac{\partial T}{\partial r} \right) + \frac{1}{r} \frac{\partial}{\partial \theta} \left( \frac{k}{r} \frac{\partial T}{\partial \theta} \right) + \frac{\partial}{\partial z} \left( k \frac{\partial T}{\partial z} \right) \quad (9)$$

In the 2D  $r-\theta$  model, the heat equation simplifies by removing the  $z$ -polar coordinate term.

As already mentioned, the temperature distribution in Eq. 6 will be dependent on the azimuthal and axial geometries because of the addition of thermocouples and holes.

### 3.3 The Weak Form Used in the Pellet-Pellet Gap

A weak form of the differential equations can be used to account for physical phenomena (appropriate values for  $\sigma$  and  $\varepsilon$ ) that apply to a surface as a more robust technique [22]. Hence, the oxygen transport in the fuel matrix equation in Eq. 1, and the gas diffusion equation in Eq. 5, can be recast as an equality of integrals, thereby reducing the order of the equations by one degree. This is accomplished by integration by parts. This eliminates the need to make very thin domains in the 3D model with a very fine mesh (which would demand considerable computation expense). In a similar treatment conducted in [18], and theory discussed in [22], weak form terms are derived for the gas phase transport equation, Eq. (5, while pulling  $c_g$  out of the time differential yields:

$$\varepsilon c_g \frac{\partial q}{\partial t} = \frac{\varepsilon \nabla}{\tau^2} \cdot (c D_g \nabla q) + \sigma R_f^{react} \quad (10)$$

In terms of the pellet-pellet gap (ppg), and where the tortuosity is unity, we can write Eq. 10 as:

$$\varepsilon_{ppg} c_g \frac{\partial q}{\partial t} = \varepsilon_{ppg} \nabla \cdot (c D_g \nabla q) + \sigma_{ppg} R_f^{react} \quad (11)$$

Equation 11 can be expressed in the more general form,

$$\varepsilon_{ppg} g \frac{\partial u}{\partial t} + \varepsilon_{ppg} \nabla \cdot \Gamma = F \quad \rightarrow \quad \varepsilon_{ppg} g V \frac{\partial u}{\partial t} + \varepsilon_{ppg} V \nabla \cdot \Gamma = VF \quad (12)$$

which is then multiplied by a test function  $V$ , where  $g$  replaces  $c_g$ ,  $u$  replaces  $q$ ,  $\Gamma$  replaces  $c D_g \nabla q$ , and  $F$  replaces  $\sigma_{ppg} R_f^{react}$ . Integrating Equation (12) over  $\Omega$  one obtains:

$$\int_{\Omega} \varepsilon_{ppg} g \frac{\partial u}{\partial t} V d\Omega + \int_{\Omega} \varepsilon_{ppg} V \nabla \cdot \Gamma d\Omega = \int_{\Omega} VF d\Omega \quad (13)$$

Integration by parts (i.e. the divergence theorem) [22] is:

$$\int_{\Omega} v \nabla \cdot \bar{u} d\Omega = \int_{\partial\Omega} \bar{u} v \cdot n d\sigma - \int_{\Omega} \bar{u} \cdot \nabla v d\Omega \quad (14)$$

Using Eq. (13) and Eq. (14) yields:

$$\varepsilon_{ppg} g \int_{\Omega} \frac{\partial u}{\partial t} V d\Omega + \varepsilon_{ppg} \int_{\partial\Omega} V (\Gamma \cdot n) ds - \varepsilon_{ppg} \int_{\Omega} \nabla V \cdot \Gamma d\Omega = \int_{\Omega} VF d\Omega \quad (15)$$

Therefore collecting terms provides the final relation:

$$\varepsilon_{ppg} g \int_{\Omega} \frac{\partial u}{\partial t} V d\Omega = \int_{\Omega} (\varepsilon_{ppg} \nabla V \cdot \Gamma + VF) d\Omega - \varepsilon_{ppg} \int_{\partial\Omega} V (\Gamma \cdot n) ds \quad (16)$$

The term on the L.H.S. is called the dweak term, the first term on the R.H.S. is called the weak term and the last term on the right is called the constraint, which is set to zero. Substituting back the values for  $F$ ,  $\Gamma$ ,  $g$  and  $u$  the weak terms in COMSOL Multiphysics format can be given as:

$$\begin{aligned} \text{dweak term:} & \quad q\_test * c_g * q\_time * \epsilon_{ppg} \\ \text{weak term:} & \quad q\_test * \sigma_{ppg} * R_{react\_fuel} - \epsilon_{ppg} * q_{Ty\_test} * c_{Dg} * q_{Ty} - \\ & \quad \epsilon_{ppg} * q_{Tz\_test} * c_{Dg} * q_{Tz} \end{aligned} \tag{17}$$

A similar treatment is performed to derive the weak terms for Equation 1 for the oxygen transport in the fuel matrix:

$$\begin{aligned} \text{dweak term:} & \quad X_{dev\_test} * X_{dev\_time} \\ \text{weak term:} & \quad X_{dev\_test} * \sigma_{ppg} * R_{react\_fuel} / c_u - \\ & \quad X_{dev} q_{Ty\_test} * D_{O2} * (X_{dev} q_{Ty} + X_{dev} * T_{star} / T^2 * q_{Ty}) - \\ & \quad X_{dev} q_{Tz\_test} * D_{O2} * (X_{dev} q_{Tz} + X_{dev} * T_{star} / T^2 * q_{Tz}) \end{aligned} \tag{18}$$

## 4. Model Results and Discussion

The model equations discussed in 3 are solved with COMSOL Multiphysics software [23]. All fuel oxidation models include a defective sheath boundary or surface. Sheath defective sizes in the models were selected so that they produce maximum stoichiometric deviation results ( $x$  or  $X_{dev}$ ) for a simulated heating time no greater than two weeks. Although steady state results are not fully achieved in two weeks, this period of time is considered an optimistic upper limit for the lifespan of the heater element.

### 4.1 2D Radial Cross Section of Test Pellet with Heating Element and Fuel Oxidation Model Results

The fuel oxidation model [1] was applied in a 2D  $r$ - $\theta$  model (a pellet cross section). Included in the model are the temperature dependant thermal conductivity properties of the test fuel element, the three different thermocouple materials, the central heater wire, and the protective materials for the heater (e.g, Ir,  $Al_2O_3$  or  $HfO_2$ ). Figure 5 depicts the locations of the heater element, defect boundary, gas diffusion domain and thermocouples. The defect is 1-mm wide. The end portion of the gas-diffusion domain is defined where the fuel changes from a cracked to a non-cracked region, i.e. where no gas diffusion can occur.

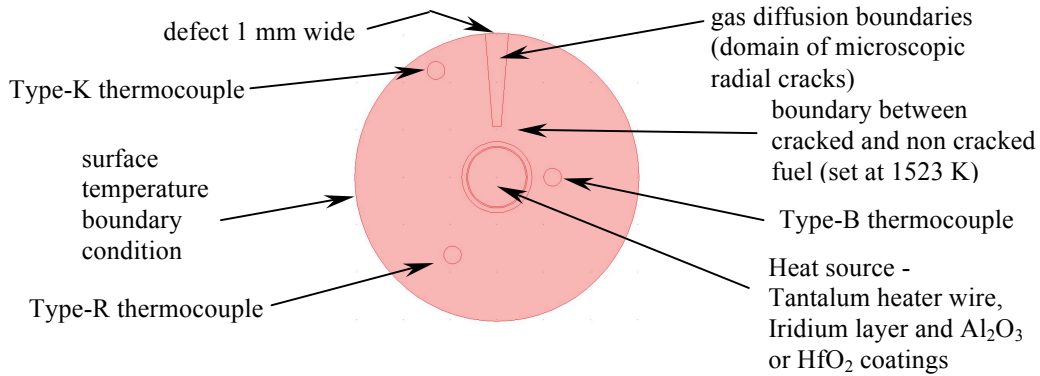


**Figure 5: Cross section of fuel pellet with a defect and heater element, hafnia or zirconia layers, Type K (nickel-chromium-aluminum), Type R (platinum-rhodium) and Type B (platinum-rhodium) thermocouples [24].**

The model was run for a heating time of two weeks. The pellet surface temperature was set to 300°C. The power in the tantalum heater wire and the iridium protective coating was set so the temperature at the Ta-Ir interface is a hundred degrees below the eutectic temperature of 1953°C, i.e. 1853°C [16]. This temperature is selected to prevent failure of the iridium coating.

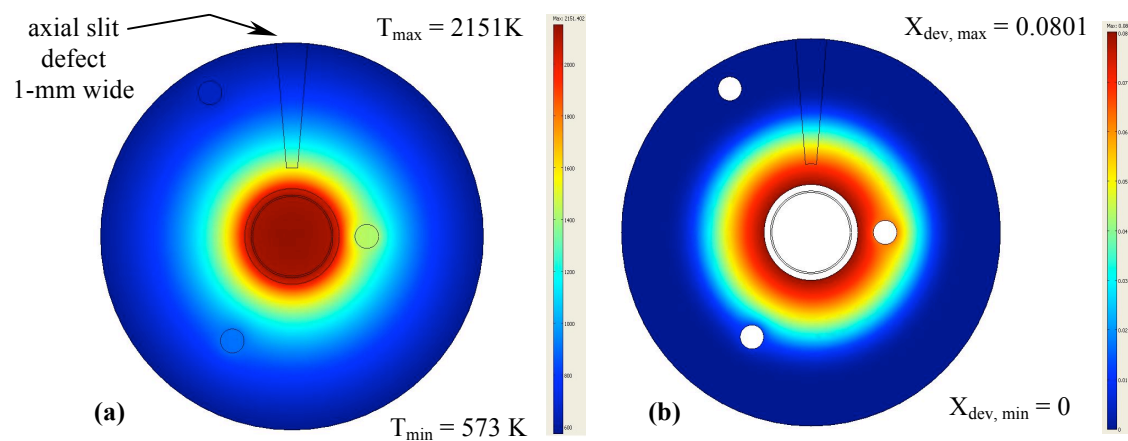


**Figure 6: (a) Temperature distribution and (b) oxygen stoichiometric deviation distribution in the UO<sub>2</sub> test pellet matrix for a 2-week heating time.**

The oxygen stoichiometric deviation predictions using the 2D  $r$ - $\theta$  model, after 1 and 2 weeks of heating, are summarized in Table 1. Hafnia is a better thermal insulator than alumina so its thickness was reduced to 0.1-mm in order that the temperature at the UO<sub>2</sub> surface would be as high as possible. The azimuthal variation in the temperature as well as the  $X_{dev}$  results are shown in Figure 6 (a) and (b). The linear power required to attain the maximum temperature feasible at the interface of the heating element and inner surface of UO<sub>2</sub> pellets is 24 kW m<sup>-1</sup> assuming that a direct current is used.

**Table 1: Inner surface temperature, required heater power and corresponding maximum oxygen stoichiometric deviation results using a 2D  $r-\theta$  model, with either an alumina or hafnia insulative layer.**

Material selection and dimensions	Temperature at inner surface of $\text{UO}_2$ pellet (3-mm diameter) [ $^{\circ}\text{C}$ ]	Power applied in Ta and Ir conductors [ $\text{kW}\cdot\text{m}^{-1}$ ]	Maximum oxygen stoichiometric deviation in $\text{UO}_{2+x}$ test pellet	
			1 week of heating time	2 weeks of heating time
1.35-mm dia. Ta, 0.05-mm Ir, 0.1-mm thick <i>hafnia</i>	1674	22.7	0.058	0.070
1.25-mm dia. Ta, 0.05-mm Ir, 0.2-mm thick <i>alumina</i>	1777	24	0.068	0.080

The results presented in Table 1 assume an infinite length slit defect using the 2D  $r-\theta$  model (see Figure 4). This conservative defect geometry is used here to obtain a preliminary estimate of the fuel temperature distribution and heater power. Hafnia is considered in these calculations for comparison purposes. Although hafnia has a lower thermal conductivity than alumina, its higher melting temperature may increase stability.

#### 4.2 Oxidation of Partial and Full Length 3D Fuel Element Models

Solution of the fuel oxidation model in a 3D geometry represents a much more realistic solution than the 2D model analysis since the defect size is accurately defined in all three dimensions. Consider a line defect that is 1-mm wide and 20-mm long (a total defect area of  $20\text{-mm}^2$ ); a defect geometry believed to be easily implemented in the out-reactor experiment. This type of defect has a 3D geometry as illustrated in Figure 7 (a). It is of note that a partial length (8-cm) fuel element is modelled to reduce the computation time and memory requirements (i.e. the partial length model is 16-cm long). The application of symmetry requires that only one quarter of the fuel element need to be modelled. The oxygen stoichiometric deviation prediction, after one week of heating, with an inner  $\text{UO}_2$  surface temperature of  $1750^{\circ}\text{C}$ , an outer surface

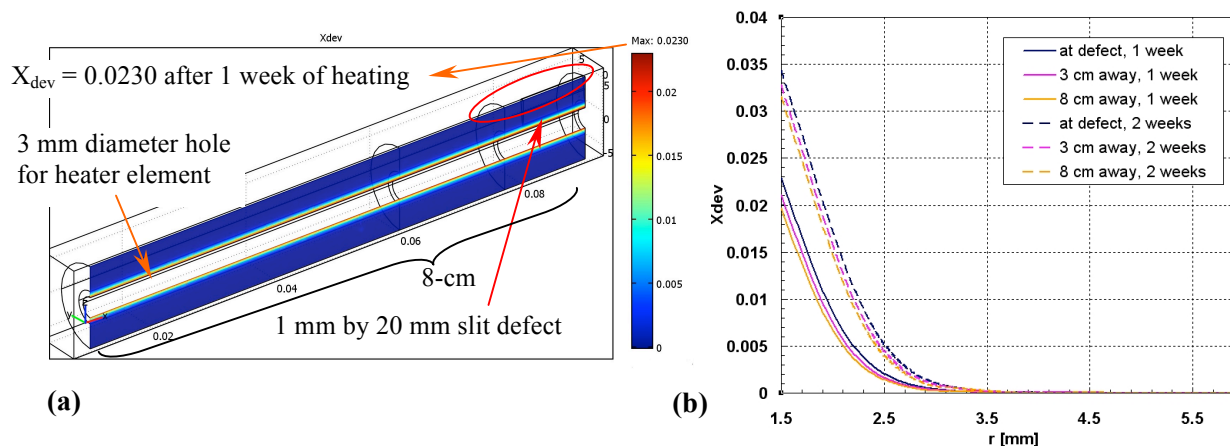


**Figure 7: (a) Isometric view of 3D model oxygen stoichiometric deviation result in an 8-cm long fuel element (representative of a 16-cm long fuel element) where the defect is a 1-mm wide and 20-mm long slit and (b) Oxygen stoichiometric deviation results vs. the radial position at three axial locations away from the defect for 1 and 2-week heating durations.**

temperature of 300°C and a 1-mm wide by 20 mm long (i.e. 0.5-mm wide by 10-mm long) slit defect, is illustrated in Figure 7 (a).

The highest stoichiometric deviation occurs near the heated fuel surface. The predicted oxidation is highest near the defect than further away from the defect as illustrated in Figure 7 (b). The maximum stoichiometric deviation ( $X_{dev}$ ) after a week of heating at these conditions is 0.0230. The oxygen concentration is highest at the inner heated surface of the pellet and there is a noticeable axial variation. After an additional week of heating the maximum stoichiometric deviation increases by 49% under and near the defect location.

The 3D model can be applied to estimate the maximum stoichiometric deviation for a number of slit defects of varying lengths. The results obtained for 1-mm wide by 20, 25 and 30-mm long slit defects are summarized in

Table 2. These models do not include a 'full' geometrical crack representation in the fuel under the defect site, instead the fuel porosity,  $\epsilon$ , is used to describe the average crack volume to fuel volume ratio in hydrogen gas diffusion equation (Eq. 8).

**Table 2: Summary of 3D model maximum oxygen stoichiometric deviation results under the defect site for 1-mm wide slit defects with varying lengths. Results tabulated for 16-cm long fuel stack model with an inner  $UO_2$  surface temperature of 1750°C and an outer surface temperature of 300°C.**

Defect Geometry Partial length (16-cm long)	Maximum $X_{dev}$	
	1 week of heating	2 weeks of heating
1-mm x 20-mm	0.0230	0.0343
1-mm x 25-mm	0.0266	0.0388
1-mm x 30-mm	0.0297	0.0427

As expected, the greater the defect surface area, the greater the extent of fuel oxidation.

Figure 8 provides fuel oxidation results for a full length fuel element that is 48-cm in length (24-cm long model).

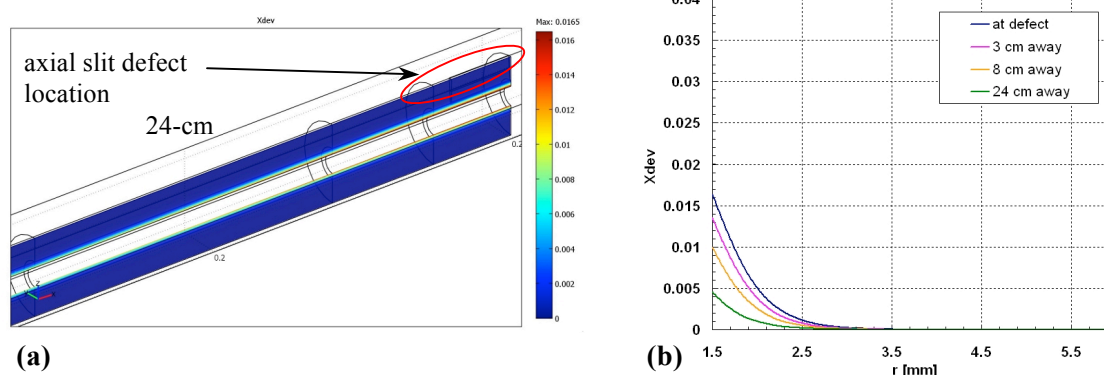


Figure 8: (a) Isometric axial cross section view of oxygen stoichiometric deviation in a full length fuel element model (48-cm) and (b) oxygen stoichiometric deviation vs. radial position in the test fuel pellet at several locations along fuel element after one-week heating. Table 3 summarizes the oxidation predictions for the full length, 48-cm long, fuel elements for a 3D simulation. Only the results for 1-mm wide by 20-mm long slit geometry was computed because of the computational expense for this calculation.

**Table 3: Maximum oxygen stoichiometric deviation results for 1-mm wide and 20-mm long slit defect in a full length 3D fuel element under the defect site.**

Defect Geometry	Maximum $X_{dev}$	
	1 week of heating	2 weeks of heating
1-mm x 20-mm	0.016	0.023

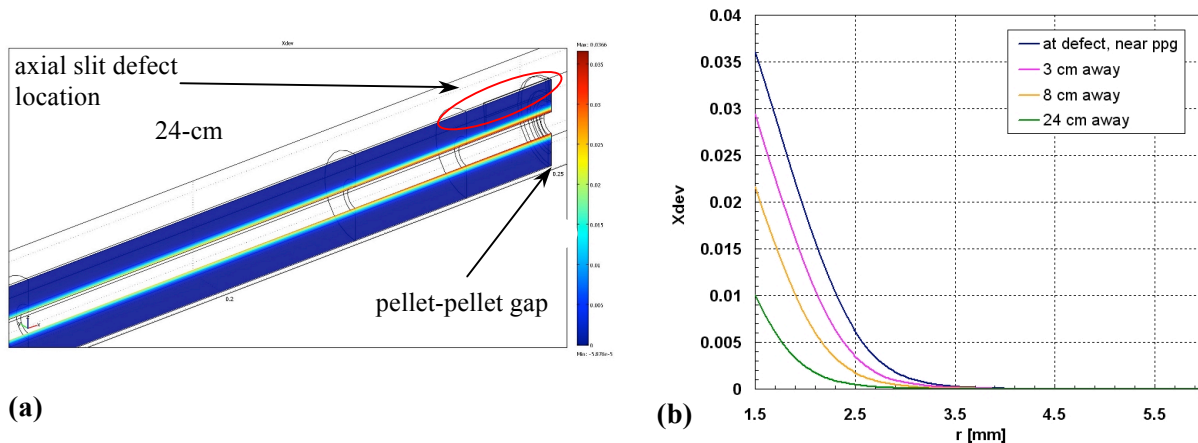
A comparison of the results in

Table 2 and Table 3, shows that that the full length model produces a lower maximum oxygen stoichiometric deviation. This is expected since more oxygen is needed to achieve the same level of fuel oxidation in the full-length model compared to the partial-length model. A heating temperature of 1750°C at the  $UO_2$  inner 3-mm diameter surface was selected based on the power and temperature results in Section 4.1.

### 4.3 Oxidation of 3D Fuel Element with Gas Phase Transport and Oxidation Weak Form Terms in the Pellet-Pellet Gap Under the Axial Slit Defect Site

In this model a pellet-pellet gap is included in the 3D model. It is conceivable that a gap may appear between two pellets under a sheath defect, allowing steam to more easily enter into this region. This gap is assumed to be present under the 1-mm wide by 20-mm long axial slit defect. Weak form terms for both gas transport and oxidation are defined on the pellet-pellet gap surfaces.  $\sigma_{ppg}$  (pellet-pellet gap) was taken as the ratio of the surface area of a pellet cross section to the volume of the whole fuel element and  $\epsilon$  (fuel porosity) is assumed to be unity. Only the surface area of one pellet cross section is considered. The width of the gap does not play a role in this model, though it may be an important consideration in future models. The depth of the pellet gap was pre-set to 3.67-mm below the pellet surface (or at  $r = 2.4$ -mm). This position is slightly above the plastic to elastic boundary location. In model analysis of thermal expansion (not presented here) it was observed that the central surfaces between pellets may come into physical contact.

Figure 9 (a) provides an axial cross section of the oxygen stoichiometric deviation distribution, and Figure 9 (b) provides radial profiles of the oxygen stoichiometric deviation at four different axial positions.



**Figure 9: (a) Isometric axial cross section view of oxygen stoichiometric deviation in a full length fuel element model (48-cm) with a pellet-pellet gap under the defect site, and (b) oxygen stoichiometric deviation vs. radial position in the test fuel pellet at several locations along fuel element after one-week heating.**

The oxygen stoichiometric deviation decreases as the distance from the defect increases. The blue curve shows that the oxygen stoichiometric deviation could be as high as  $\text{UO}_{2.036}$  near the defect site and near the heater element in one week of heating with consideration of a pellet-pellet gap under the defect site. Post experiment techniques can provide oxygen potential values at various locations in the fuel test pellets to validate the predictions. Table 4 provides a preliminary result for maximum oxygen stoichiometric deviation in a full-length fuel element when fuel oxidation occurs in the presence of a pellet-pellet gap under the sheath defect location.

**Table 4: Maximum stoichiometric deviation in a full-length fuel element after one and two weeks of heating in a 3D model with a pellet-pellet gap under the defect site.**

Defect Geometry Full length model (48-cm)	Maximum $X_{\text{dev}}$	
	1 week of heating	2 weeks of heating
1-mm x 20-mm with a pellet-pellet gap under the defect	0.036	0.047

A comparison of results in Table 3 and Table 4 or Figures 8b and 9b shows an increase in stoichiometric deviation when considering the possibility of an open gap between two pellets under a defect site.

The inclusion of the pellet-pellet gap under a defect in the 3D fuel oxidation model using weak form equations on the relevant surfaces may prove to be useful in interpreting the out-reactor experimental results. This phenomenon, among possible others, may help to explain the lower predictions of 3D model results where a pellet gap was not considered [18]. It should be noted that the 2D model defect sizes in the Higgs model [18] were considerably larger (greater than a factor of ten) than actual defect sizes in real fuel defected fuel element experiments. Current work is continuing the improvement the 3D fuel oxidation model. Out-reactor experiments will thus help benchmark the fuel-oxidation model.

## 5. Conclusions

In this paper, 2D and 3D simulations of fuel oxidation behaviours were presented for a planned out-reactor experiment. The 3D model provides a more realistic result for predicting oxygen stoichiometric deviation in  $\text{UO}_2$  fuel pellets because the defect size is specifically defined. A 1-mm wide slit of varying lengths was investigated. As expected, the 3D model results indicated that increased defect length (i.e. increased defect surface area) yields a maximum oxygen stoichiometric deviation in the fuel element.

The results of this work can be used to estimate the appropriate sheath defect surface area that must be used for the out-reactor test. From the model results, it is concluded that within one week of heating, a defective fuel element will have enough fuel oxidation for observation in post examination. The model without pellet-pellet gap treatment also shows that an additional week of heating will increase the maximum oxygen stoichiometric deviation by 49% in the partial length model and 44% in the full length model.

A 2D  $r$ - $\theta$  model, considering information on the thermal conductivities as function of temperature for all relevant materials, was used to estimate the required linear power and temperature profile of the test pellets in the out-reactor experiment. The results of this model

were found to be highly dependent on material selection and the material geometry. Material selection and suitable dimensions are thus suggested in this paper.

The inclusion of a pellet-pellet gap was investigated in the 3D model. These preliminary results show that if such a gap is present under a deliberate sheath defect, an increased fuel oxidation level may occur.

Future work includes improving the fuel oxidation model by an enhanced representation of fuel cracks under the sheath defect. Inclusion of a pellet-pellet gap under a defect in model will also be further investigated.

### Acknowledgements

The authors would like to acknowledge the useful comments provided by Tony Williams from Chalk River Laboratories, Atomic Energy Canada Ltd. in preparation of this CNS student paper.

---

### References

- [1] J.D. Higgs, B.J. Lewis, W.T. Thompson and Z. He, "A conceptual model for the fuel oxidation of defective fuel", *Journal of Nuclear Materials*, 366 (2007) 99.
- [2] B.J. Lewis, F.C. Iglesias, D.S. Cox and E. Gheorghiu, "A model for fission gas release and fuel oxidation behaviour for defected UO<sub>2</sub> fuel elements", *Nuclear Technology*, 92 (1990) 353.
- [3] B.J. Lewis, R.D. MacDonald, N.V. Ivanoff and F.C. Iglesias, "Fuel performance and fission product release studies for defected fuel elements", *Nuclear Technology*, 103 (1992) 220.
- [4] D.R. Olander, "Oxidation of UO<sub>2</sub> by High-Pressure Steam", *Nuclear Technology*, 74 (1986) 215.
- [5] D.R. Olander, Y.S. Kim, W. Wang and S.K. Yagnik, "Steam oxidation of fuel in defective LWR rods", *Journal of Nuclear Materials*, 270 (1999) 11.
- [6] B.J. Lewis, B. Szpunar and F.C. Iglesias, "Fuel oxidation and thermal conductivity model for operating defective fuel rods", *Journal of Nuclear Materials*, 306 (2002) 30.
- [7] B.J. Lewis, W.T. Thompson, F. Akbari, D.M. Thompson, C. Thurgood and J. Higgs, "Thermodynamic and kinetic modelling of the fuel oxidation behaviour in operating defective fuel", *Journal of Nuclear Materials*, 328 (2004) 180.
- [8] H. Matzke, "Gas release mechanisms in UO<sub>2</sub> - A critical review", *Radiation Effects*, 53 (1980) 219.
- [9] W. Hüttig, H. Enker and M. Forberg, "In-Core surveillance of defective PWR fuel elements in the case of fuel-to-water contact", *Journal of Nuclear Materials*, 175 (1990) 147.
- [10] K. Une, M. Imamura, M. Amaya and Y. Korei, "Fuel oxidation and irradiation behaviours of defective BWR fuel rods", *Journal of Nuclear Materials*, 223 (1995) 40.
- [11] M. Limbäck, M. Dahlbäck, L. Hallstadius, P.M. Dalene, H. Devold, C. Vitanza, W. Wiesennack, H. Jenssen, B.C. Oberländer, I. Matsson and T. Andersson, "Test-reactor study of the phenomena involved in secondary fuel degradation", Proceedings of the 2004 International Meeting on LWR Fuel Performance, Orlando, Florida, September 19-22, 2004, Paper 1045.
- [12] B. Cheng, B.C. Oberländer, W. Weisenack, S. Yagnik and J. Turnbull, "An in-reactor

- 
- simulation test to evaluate root cause of secondary degradation of defective BWR fuel rod”, Zirconium in the nuclear industry: 13<sup>th</sup> International Symposium, ASTM STP 1423 (2002) 616.
- [13] A. Viktorov and M. Couture, Regulatory Activities in the Area of Fuel Safety and Performance, Fuelling A Clean Future, 9th International CNS Conference on CANDU Fuel, September 18-21, 2005.
- [14] R.A. Verrall, Z. He and J. Mouris, “Characterization of Fuel Oxidation in Rods with Clad-Holes”, *Journal of Nuclear Materials*, 344 (2005) 240-245.
- [15] M. Oguma, “Cracking and relocation behaviour of nuclear fuel pellets during rise to power”, *Nuclear Engineering and Design*, 76 (1983) 35.
- [16] T. Massalski Editor-in-Chief, American Society for Metals, Binary Alloy Phase Diagrams, Vol. 2. Ohio USA, 1986.
- [17] P.G. Lucuta, H. Matzke and R.A. Verrall, “Microscopic features of SIMFUEL - simulated high-burnup UO<sub>2</sub> based nuclear fuel”, *Journal of Nuclear Materials*, 178 (1991) 48.
- [18] J. Higgs, Modelling Oxidation Behaviour in Operating Defective Nuclear Reactor Fuel Element, Department of Chemistry and Chemical Engineering, Royal Military College of Canada, PhD Thesis, 2006.
- [19] Y. Sumi, L.M Keerand, and S. Nemat-Nasser, “Thermally induced radial cracking in fuel element pellets”, *Journal of Nuclear Materials* 96 (1981) 147.
- [20] C. Bernaudat, “Mechanical behaviour modelling of fractured nuclear fuel pellets”, *Nuclear Engineering and Design*, 156 (1995) 373.
- [21] D.R. Olander, Fundamental Aspects of Nuclear Reactor Fuel Elements, University of California, Technical Information Center, Energy Research and Development Administration, 1976.
- [22] William B.J. Zimmerman, Multiphysics Modelling with Finite Element Methods, World Scientific Publishing Co. Pte. Ltd., London, 2006.
- [23] COMSOL Multiphysics Version 3.5a finite element modeling and simulation commercial software, [www.comsol.com](http://www.comsol.com).
- [24] Omega Engineering Inc., [www.omega.com/temperature/Z/zsection.asp](http://www.omega.com/temperature/Z/zsection.asp)